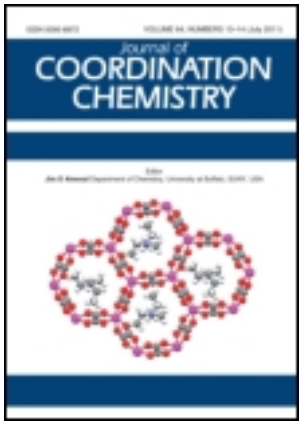

Journal of Coordination Chemistry
Publication details, including instructions for authors and subscription information:
http://www.tandfonline.com/loi/gcoo20

Synthesis and photovoltaic properties of polymeric metal complexes containing 8-hydroxyquinoline as dye sensitizers for dye-sensitized solar cells

Lirong Zhang [a], Gaojun Wen [a], Qian Xiu [a], Lihui Guo [a], Jinyan Deng [a] & Chaofan Zhong [a]

[a] Key Laboratory of Environmentally Friendly Chemistry and Applications of Ministry of Education, College of Chemistry, Xiangtan University, Xiangtan, Hunan 411105, PR China

Version of record first published: 05 Apr 2012

To cite this article: Lirong Zhang, Gaojun Wen, Qian Xiu, Lihui Guo, Jinyan Deng & Chaofan Zhong (2012): Synthesis and photovoltaic properties of polymeric metal complexes containing 8-hydroxyquinoline as dye sensitizers for dye-sensitized solar cells, Journal of Coordination Chemistry, 65:9, 1632-1644

To link to this article: http://dx.doi.org/10.1080/00958972.2012.677532

Journal of Coordination Chemistry
Vol. 65, No. 9, 10 May 2012, 1632–1644

Taylor & Francis
Taylor & Francis Group

Synthesis and photovoltaic properties of polymeric metal complexes containing 8-hydroxyquinoline as dye sensitizers for dye-sensitized solar cells

LIRONG ZHANG, GAOJUN WEN, QIAN XIU, LIHUI GUO, JINYAN DENG and CHAOFAN ZHONG*

Key Laboratory of Environmentally Friendly Chemistry and Applications of Ministry of Education, College of Chemistry, Xiangtan University, Xiangtan, Hunan 411105, PR China

(*Received 4 September 2011; in final form 28 February 2012*)

Four new donor–acceptor type polymeric metal complexes (**P1**, **P2**, **P3**, and **P4**) with the same Cd(II) complex in side chain and different conjugated backbone structures were synthesized by Yamamoto coupling and applied in dye-sensitized solar cells (DSSCs) as photosensitizers. The photophysical, electrochemical, and thermal properties were investigated in detail, showing that conjugated backbone containing fluorene improved intramolecular charge transfer and increased generation of photocurrent. The highest power conversion efficiency of 0.56% ($J_{sc} = 1.63\,mA\,cm^{-2}$, $V_{oc} = 0.69\,V$, $FF = 0.50$) was obtained with a DSSC based on **P3** under simulated air mass 1.5 G solar irradiation, which shows a new strategy to design photosensitizers for DSSCs.

Keywords: Donor–acceptor; Dye-sensitized solar cells; Polymeric metal complexes; Fluorene

1. Introduction

Increasing energy demands and concerns about global warming have encouraged scientists to develop cheap and easily accessible renewable energy sources. In comparison with the traditional silicon-based solar cells, dye-sensitized solar cells (DSSCs) are promising photovoltaic cells due to versatile, energy-saving, and environmentally friendly nature [1]. Therefore, DSSCs have been intensively studied since the breakthrough made by O'Reagen and Grätzel in 1991 [2]. Typical dyes are ruthenium(II)–polypyridyl photosensitizers which have achieved power conversion efficiencies over 11% in standard air mass 1.5 G sunlight [3–6], but they are not ideal cost-effective and environmentally friendly photovoltaic devices. Organic dyes as an alternative to ruthenium(II) complex photosensitizers exhibit many advantages [7–9]: (1) molecular structures of organic dyes are diverse and can be easily designed and synthesized, (2) organic dyes are superior to the Ru complexes for cost and environment issues, (3) in solutions or thin films, organic dyes often show high molar extinction coefficients, (4) organic dyes exhibit higher efficiencies than Ru complexes in

*Corresponding author. Email: zhongcf798@yahoo.com.cn

Journal of Coordination Chemistry
ISSN 0095-8972 print/ISSN 1029-0389 online
http://dx.doi.org/10.1080/00958972.2012.677532

p-type DSSCs. These features make organic dyes attractive for photovoltaics and great efforts have been devoted to developing organic molecule dyes [10–12]. Some conjugated polymers used as photosensitizers in DSSCs have been reported [13–21].

Polyfluorene (PF)-based conjugated polymers have been extensively utilized in optoelectronics due to high fluorescence quantum yield, excellent hole-transporting properties [22, 23], and good film-forming properties [24, 25]. However, poor thermal stability, high-energy barrier, and blue shift of absorptions of these polymers may limit their large-scale application. These problems can be solved by incorporating electron-donor or electron-acceptor units into the main PF chain to form a donor-(π-spacer)-acceptor (D-π-A) system. Generally, D-π-A systems are the basic structure for designing organic sensitizers due to effective light induced intramolecular charge transfer (ICT) [26–30], which results in fast charge separation yet extremely slow charge recombination, holding promise for constructing molecular optoelectronic devices.

8-Hydroxyquinoline (8-HQ) is one of the most important chelators for metal ions and has been widely used. An electron-donating group in the 5- or 7-position of 8-hydroxyquinoline causes a red shift in absorption and emission spectra. Although reports of their application as dye sensitizers for DSSCs are rare, chemical modifications between PFs and 8-HQ may satisfy application requirements to suppress charge recombination and improve open-circuit photovoltage (V_{oc}) [31–33].

In this article, we have designed and synthesized four D–A dyes with the same Cd(II) complex in the side chain as electron acceptor with different conjugated backbones containing fluorene, alkoxy benzene, or carbazole as the electron donor. The dyes are tuned by co-monomers in the backbone chain to change the photophysical and electrochemical properties and thus improve the photovoltaic performance. Optical, photovoltaic, and thermal properties of the four polymeric metal complexes were investigated.

2. Experimental

2.1. *Materials*

$NiCl_2(PPh_3)_2$, fluorene, 8-hydroxyquinoline, Pb/C, and *N*-bromosuccinimide (NBS) were obtained from Aldrich Chemical Company and used as received. Ethanol was dried through molecular sieves and freshly distilled prior to use. *N*,*N*-dimethylformamide was dried by distillation over CaH_2. The other materials were of commercial grade and used as received. 5-Formyl-8-hydroxyquinoline [34], 5-formyl-8-tosyloxyquinoline [35], and 2,7-dibromofluorene [36] were prepared according to literature procedure. All chemicals used were of analytical grade. Solvents were purified with conventional methods.

2.2. *Instruments and measurements*

Nuclear magnetic resonance ^1H NMR spectroscopy was performed in $CDCl_3$ and recorded on a Bruker NMR 400 spectrometer using TMS (0.00 ppm) as the internal reference. FT-IR spectra were obtained on a Perkin-Elmer Spectrum One Fourier transform infrared spectrometer with KBr discs. Thermogravimetric analyses (TGA)

were run on a Shimadzu TGA-7 Instrument in nitrogen at a heating rate of 20°C min^{-1} from 25°C to 900°C. Differential scanning calorimetry (DSC) was performed on materials using a Perkin-Elmer DSC-7 thermal analyzer in nitrogen at a heating rate of 20°C min^{-1} from 25°C to 300°C. UV-Vis spectra were taken on a Lambda 25 spectrophotometer. Photoluminescence (PL) spectra were taken on a Perkin-Elmer LS 55 luminescence spectrometer with a xenon lamp as the light source. Elemental analysis for C, H, and N was carried out using a Perkin-Elmer 2400 II instrument. Cyclic voltammetry (CV) was conducted on a CHI chi630c Electrochemical Workstation in a 0.1 mol L^{-1} $[Bu_4N]BF_4$ (Bu = butyl) DMF solution at a scan rate of 100 mV s^{-1} at room temperature. The working electrode was a glassy carbon rod, the auxiliary electrode was a Pt wire electrode, and saturated calomel electrode (SCE) was used as reference electrode. Gel permeation chromatography (GPC) analysis was done on a WATER 2414 system with DMF as an eluent (1.0 mL min^{-1}) at 80°C.

2.3. *General procedure for preparation and testing of DSSCs*

The FTO glass (fluorine doped SnO_2, sheet resistance 14 X/sq, transmission >90% in the visible) was first cleaned in a detergent solution using an ultrasonic bath for 15 min and then rinsed with water and ethanol. The washed FTO glass was immersed in 40 mmol L^{-1} aqueous $TiCl_4$ solution at 70°C for 30 min and then washed with water and ethanol. Titania paste was prepared from 12 g of P25 (Degussa AG, Germany) following a literature procedure [37] and added with 3.6 mL of 1% magnesium acetate solution [38]. Then the paste was deposited onto the FTO glass by the sliding glass rod method. The TiO_2-coated FTO glass was sintered at 450°C for 30 min in air. The sintered film was treated with 40 mmol L^{-1} $TiCl_4$ aqueous solution at 45°C for 30 min and annealed again at 450°C for 30 min. After the film was cooled to 80°C, the TiO_2 electrodes were soaked in 0.5 mmol L^{-1} samples dyes **P1–P4** in DMF solution and maintained under dark overnight. 3-Methoxypropionitrile solution containing LiI (0.5 mol L^{-1}), I_2 (0.05 mol L^{-1}), and 4-tert-butylpyridine (TBP) (0.5 mol L^{-1}) was used as the electrolyte. A platinized FTO glass used as counter electrode was prepared by sputtering 200 nm Pt film on FTO glass. The dye-coated semiconductor film was illuminated through a conducting glass support without a mask. Photoelectron chemical performance of the solar cell was measured using a Keithley 2602 Source meter controlled by a computer. The cell parameters were obtained under an incident light intensity of 100 mW cm^{-2}, which was generated by a 500 W Xe lamp passing through an AM 1.5 G filter with an effective area of 0.16 cm^2.

2.4. *Synthesis*

The synthetic routes of the monomers and polymeric metal complexes are shown in scheme 1.

2.4.1. Synthesis of 5-formyl-8-hydroxyquinoline (1). Compound **1** was synthesized according to the published literature [34]. Yield: 24%. ^{1}H NMR ($CDCl_3$, d, ppm): 10.14 (s, 1H), 9.67–9.69 (d, 1H), 8.86–8.87 (t, 1H), 7.99–8.00 (d, 1H), 7.64–7.67 (m, 1H), 7.25–7.29 (t, 1H).

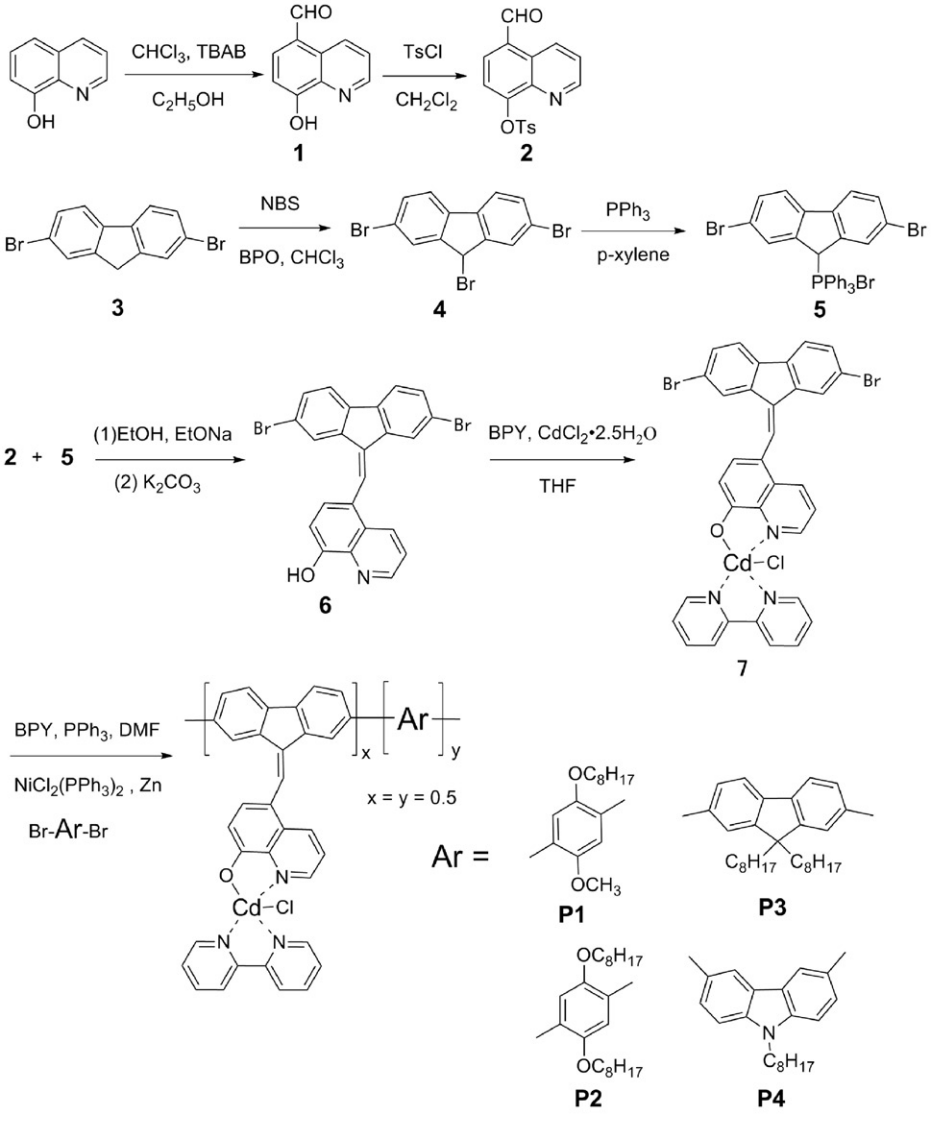

Scheme 1. Synthesis of the co-monomers and polymeric metal complexes **P1–P4**.

2.4.2. Synthesis of 5-formyl-8-tosyloxyquinoline (2). Compound **2** was synthesized according to the published literature [35]; **1** (2.61 g, 15 mmol) was dissolved in dichloromethane (80 mL) and TsCl (3.2 g, 18 mmol) was added in one portion under the ice-water and then stirred at ambient temperature. After 12 h, the solution was poured into cool water. The organic layer was collected and dried over anhydrous $MgSO_4$; removal of solvent gave yellow solid (5.12 g, 98%). ^{1}H NMR ($CDCl_3$, d, ppm): 10.26 (s, 1H), 9.75 (d, 1H), 9.55–9.61 (d, 1H), 8.00–8.06 (d, 1H), 7.80–7.82 (d, 1H), 7.58–7.59 (d, 2H), 7.40–7.42 (d, 2H), 7.35–7.40 (d, 1H), 0.85–0.88 (t, 3H).

2.4.3. Synthesis of 2,7-dibromofluorene (3). Compound **3** was synthesized according to the literature [36]. Fluorene (8.25 g, 50 mmol) and *n*-bromosuccinimide (17.8 g, 0.1 mol) were added into 100 mL acetic acid; then 3.5 mL HBr was added with stirring under nitrogen, and the reaction was continued 24 h at 90°C. Yellow solid was collected by filtration and washed by methyl alcohol, recrystallized from ethanol giving white solid (6.69 g, yield 81%); m.p.: 201–202°C. ^{1}H NMR ($CDCl_3$, d, ppm) 7.55 (d, 4H), 7.44 (d, 2H), 4.15 (s, 1H).

2.4.4. Synthesis of 2,7,9-tribromofluorene (4). Compound **4** was synthesized according to the published literature [39]. A mixture of **3** (10.02 g, 31 mmol), *N*-bromosuccinimide (NBS) (6.04 g, 31 mmol), and carbon tetrachloride (300 mL) was placed in a 500 mL round bottom flask. The mixture was refluxed and benzoyl peroxide was added as initiator. The mixture was irradiated under IR lamp for 30 min and continued to reflux for 4 h. The product was washed twice with dilute sodium bicarbonate, twice with water, and once with saturated sodium chloride. The combined organic layer was dried over anhydrous $MgSO_4$, filtered and evaporated to get the crude product. The crude product was recrystallized by ethanol to obtain white solid (7.46 g, 58%). ^{1}H NMR (400 MHz, $CDCl_3$, δ, ppm): 7.70 (s, 2H), 7.58–7.62 (d, 2H), 7.51–7.53 (d, 2H), 5.56 (s, 1H). Anal. Calcd for [$C_{13}H_7Br_3$]: C, 38.75; H, 1.75. Found: C, 38.61; H, 1.72.

2.4.5. Synthesis of 2,7-dibromo-9-triphenylphosphoniomethylbromo-fluorene (5). Compound **5** was synthesized according to the literature [40]. A solution of **2** (8.11 g, 20 mmol) and triphenylphosphine (6.30 g, 24 mmol) in 150 mL of dried 1,4-xylene was refluxed for 12 h. The reaction system was then allowed to cool to room temperature and the white precipitate was collected by filtration, washed with dried ether and acetone repeatedly, followed by drying; white solid was obtained (10.44 g, 81%). ^{1}H NMR (400 MHz, $CDCl_3$, δ, ppm): 7.87 (s, 2H), 7.65–7.72 (m, 15H), 7.55 (d, 2H), 7.47 (d, 2H), 6.62 (s, 1H). Anal. Calcd for [$C_{31}H_{22}Br_3P$]: C, 55.97; H, 3.33. Found: C, 55.82; H, 3.29.

2.4.6. Synthesis of 2,7-dibromo-9-2-(8-hydroxyquinoline)vinylfluorene (DB8QF) (6). Compound **6** was synthesized according to the literature [41]. Compounds **5** (3.32 g, 5 mmol) and **2** (1.56 g, 5 mmol) were dissolved in 200 mL of absolute alcohol. Under an ice-water bath, $NaOC_2H_5$ (2.0 g sodium in 60 mL of absolute alcohol) was added to the solution. After 30 min, the solution was stirred for 12 h at ambient temperature. Then potassium carbonate (1.05 g, 7.5 mmol) was added and refluxed for 8 h. Yellow solid was collected at the end of the condensation and washed with distilled water and icy methanol. After drying in vacuum at 45°C, the compound was obtained as light yellow solid (1.42 g, 65%). ^{1}H NMR ($CDCl_3$, δ, ppm): 8.91 (s, 1H), 7.90–7.92 (d, 1H), 7.70–7.76 (m, 2H), 7.67 (s, 2H), 7.52–7.58 (m, 4H), 7.02–7.08 (t, 2H). FT-IR (KBr, cm^{-1}): 3348 (O–H), 3105, 2952 (aromatic and vinylic C–H), 2912 (aliphatic C–H), 1583 (C=N), 1446 (C=C), 1414 (fluorene, C–H). Anal. Calcd for [$C_{23}H_{12}ONBr_2$]: C, 57.77; H, 2.53; N, 2.93. Found: C, 57.84; H, 2.61; N, 2.98.

2.4.7. Synthesis of DB8QFCd (7). Compound **7** was synthesized according to the published procedure [35]. An ethanol solution (10 mL) of $CdCl_2 \cdot 2.5H_2O$ (0.228 g,

1 mmol) was dropped into a mixed THF solution (20 mL) of **6** (0.479 g, 1 mmol) and 2,2′-bipyridine (0.156 g, 1 mmol). The reaction mixture was neutralized carefully with 1 mol L^{-1} aq sodium hydroxide until neutral to slightly acidic pH, refluxed for 6 h and then recrystallized from ethanol, filtered, washed with ethanol repeatedly and dried in vacuum at 25°C. The pale precipitate was collected (0.63 g, 81%). FT-IR (KBr, cm^{-1}): 3059, 2912, 2853 (aromatic and vinylic C–H), 1574 (C=N), 1466 (C=C), 1414 (C–N), 1096 (C–O–M), 485 (M–N). Anal. Calcd for [$C_{33}H_{20}ON_3ClBr_2Cd$]: C, 50.67; H, 2.58; N, 5.37. Found: C, 50.72; H, 2.62; N, 5.31.

2.4.8. Synthesis of 1,4-dibromo-2-methoxy-5-(octyloxy)benzene (8). Compound **8** was synthesized according to the literature [42] (yield 73%). ^{1}H NMR ($CDCl_3$, δ, ppm): 4.01–4.05 (m, 2H), 3.93 (s, 2H), 3.77 (s, 3H), 1.86–1.92 (m, 2H), 1.27–1.64 (m, 10H), 0.97 (t, 3H). Anal. Calcd for [$C_{15}H_{22}Br_2O_2$]: C, 45.71; H, 5.63; O, 8.12. Found: C, 45.82; H, 5.68; O, 8.18.

2.4.9. Synthesis of 1,4-dibromo-2, 5-bis(octyloxy)benzene (9). The procedure for **9** was similar to that of **8** giving white solid (yield 65%). ^{1}H NMR ($CDCl_3$, δ, ppm): 7.16 (s, 2H), 3.96–4.04 (m, 4H), 1.81–1.89 (m, 4H), 1.34–1.54 (m, 20H), 0.95 (t, 6H). Anal. Calcd for [$C_{22}H_{36}Br_2O_2$]: C, 53.67; H, 7.37; O, 6.50. Found: C, 53.81; H, 7.44; O, 6.55.

2.4.10. Synthesis of 2,7-dibromo-9,9-dioctyl-fluorene (10). Compound **10** was synthesized according to the literature [43] (yield 44%). ^{1}H NMR ($CDCl_3$, δ, ppm): 7.52 (d, 2H), 7.45 (d, 2H), 7.43 (d, 2H), 1.92 (m, 4H), 1.24–1.10 (m, 20H), 0.84 (t, 6H), 0.57 (m, 4H). Anal. Calcd for [$C_{29}H_{40}Br_2$]: C, 63.51; H, 7.35. Found: C, 63.62; H, 7.41.

2.4.11. Synthesis of 2,7-dibromo-9-octylcarbazole (11). Compound **11** was synthesized according to published procedure [44] (yield 75%). ^{1}H NMR ($CDCl_3$, δ, ppm): 0.97 (t, 3H), 1.28 (m, 8H), 1.33 (m, 2H), 2.01 (m, 2H), 3.90 (t, 2H), 7.28 (d, 2H), 7.56 (d, 2H). Anal. Calcd for [$C_{20}H_{23}Br_2N$]: C, 54.94; H, 5.30; N, 3.20. Found: C, 60.07; H, 5.35; N, 3.23.

2.5. *General procedure of polymeric metal complexes*

Polymeric metal complex was synthesized by the Yamamoto coupling method [41]. Compound **7** (0.340 g, 0.4 mmol), bis(triphenylphosphine), nickel(II) chloride (0.26 g, 0.4 mmol), compounds **8**–**11** (0.4 mmol), zinc (0.13 g, 2 mmol), triphenylphosphine (0.209 g, 0.8 mmol), and 2,2′-bipyridine (0.006 g, 0.038 mmol) were dissolved in DMF (15 mL) under nitrogen. Then the mixture was stirred at 90°C for 48 h. The solid was precipitated in a large excess of ethanol solution. The crude product was washed with ethanol, distilled water, and THF sequentially, then dried in vacuum at 60°C for 1 day to afford pale yellow solid in a yield of 44–56%.

Polymeric metal complex **P1**: Yield: 53%. FT-IR (KBr, cm^{-1}): 3066, 2943 (aromatic and vinylic C–H), 1561 (C=N), 1443 (C=C), 1021 (C–O–M). Anal. Calcd for [$C_{47}H_{40}O_3N_3ClCd$]: C, 66.99; H, 4.78; N, 4.99. Found: C, 67.08; H, 4.86; N, 4.96.

Polymeric metal complex **P2**: Yield: 48%. FT-IR (KBr, cm^{-1}): 3074, 2934, 2849 (aromatic and vinylic C–H), 1554 (C=N), 1429 (C=C), 1066 (C–O–M). Anal. Calcd for [$C_{55}H_{56}O_3N_3ClCd$]: C, 69.18; H, 5.91; N, 4.40. Found: C, 69.22; H, 6.03; N, 4.47.

Polymeric metal complex **P3**: Yield: 56%. FT-IR (KBr, cm^{-1}): 3067, 2929, 2851 (aromatic and vinylic C–H), 1542 (C=N), 1418 (C=C), 1018 (C–O–M). Anal. Calcd for [$C_{62}H_{60}ON_3ClCd$]: C, 73.65; H, 5.98; N, 4.16. Found: C, 73.67; H, 6.10; N, 4.21.

Polymeric metal complex **P4**: Yield: 44%. FT-IR (KBr, cm^{-1}): 3073, 2953 (aromatic and vinylic C–H), 1563 (C=N), 1452 (C=C), 1068 (C–O–M). Anal. Calcd for [$C_{53}H_{43}ON_4ClCd$]: C, 70.75; H, 4.82; N, 6.23. Found: C, 70.84; H, 4.86; N, 6.34.

3. Results and discussion

3.1. *Synthesis*

Scheme 1 outlines the synthetic routes to **6**, which was synthesized by the Wittig reaction and four polymeric metal complexes **P1–P4** which were synthesized by Yamamoto coupling protocol.

^{1}H NMR spectra (Supplementary material) of **DB8QF** (**6**) shows vinyl proton peaks at 7.03 ppm and 8.91 ppm; 7.90–7.92 ppm, 7.70–7.76 ppm, ~7.05 ppm were attributed to protons of 8-hydroxyquinoline, while protons of the fluorene ring were observed at 7.67 ppm and 7.52–7.58 ppm. There was no detectable signal for OH in $CDCl_3$ in the spectra [45].

The FT-IR spectra of **DB8QFCd** and the copolymers **P1–P4** show a sharp absorption at 1574 cm^{-1} ascribed to C=N stretch of 8-hydroxyquinoline. Absorptions at 1464, 1414 are due to C=C, C–N stretches, respectively; the peak at 1096 cm^{-1} in the IR spectra of **DB8QFCd** was attributed to coordination of 8-hydroxyquinoline with Cd^{2+} [46]. In **DB8QFCd**, a new band at 485 cm^{-1}, absent in free **DB8QF**, can be attributed to metal–nitrogen bonds [47]. Sharp bands at 2912 cm^{-1} and 2853 cm^{-1} are associated with CH_2 asymmetric and symmetric stretching vibrations, respectively, indicating that alkyl or alkoxy aromatic derivatives have been imbedded in the molecular chain. The average molecular weight of the coploymers (table 1) proves that copolymerization has taken place between the monomers and gives evidence of the success of the polymerization when taken together with the data of the elemental analysis.

GPC shows that **P1–P3** have average molecular weights of 7.89, 7.20, 9.34, and 9.83 kg mol^{-1} (9, 8, 9, and 11 repeating units on average for **P1–P4**, respectively) with

Table 1. Polymerization, thermal, and optical properties of **P1–P4**.

Polymer	$\overline{M}_n(\times10^3)$	$\overline{M}_w(\times10^3)$	PDI	T_g[a] (°C)	T_d[b] (°C)	$\lambda_{a,max}$ (nm)	$\lambda_{f,max}$ (nm)
P1	7.89	15.75	1.89	98	317	397	466
P2	7.20	11.72	1.63	92	327	389	471
P3	9.34	18.94	2.02	116	269	411	454
P4	9.83	21.13	2.15	105	335	419	449

[a]Glass transition temperature, measured from DSC traces of the polymeric metal complexes.
[b]The data were obtained from TGA of the polymeric metal complexes.

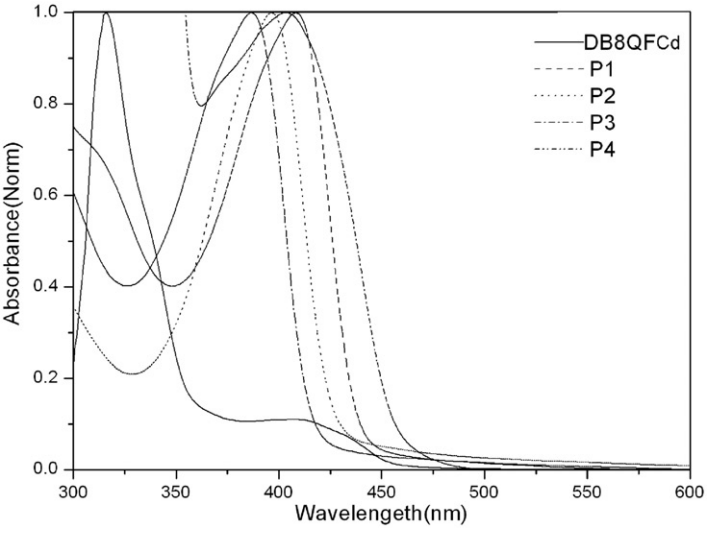

Figure 1. Normalized UV-Vis absorption spectra of the polymers in DMF (10^{-5} mol L^{-1}).

a relatively narrow polydispersity index (PDI) between 1.89, 1.63, 2.02, and 2.15 for **P1–P4**, respectively (shown in table 1). As expected, **P1–P4** were soluble in DMF, DMSO, and toluene, but present poor solubility in THF, DCM, and MeOH.

3.2. *Optical properties*

The photophysical properties of the polymers were investigated by UV-Vis and fluorescence spectroscopy in dilute DMF solution (10^{-5} mol L^{-1}). The absorption spectra of the ligand and the polymeric metal complexes are shown in figure 1 and the corresponding optical data of the polymeric metal complexes are summarized in table 1. For comparison, the absorption spectrum of **DB8QFCd** is included. Absorption spectra of the polymers exhibited similar curves with one maximum ($\lambda_{a,max}$) at 397 nm, 389 nm, 411 nm, and 419 nm, respectively, corresponding to the π–π^* transitions of the conjugated molecules. Absorption peaks of the polymers were red-shifted about 82 nm, 74 nm, 94 nm, and 104 nm in comparison with **DB8QFCd**, resulting from the lengthening of π–π conjugated main chain, boding well for their photovoltaic properties.

Fluorescence spectroscopy of polymeric metal complexes (**P1**–P4), recorded upon excitation at the maximum absorption in the UV-Vis spectra, were measured in diluted DMF solution (10^{-5} mol L^{-1}). As observed from figure 2, the maximum ($\lambda_{e,max}$) emission peaks of the polymers were 476 nm, 449 nm, 457 nm, and 469 nm, respectively. PL intensity of **P1** and **P2** were higher than that of **P3** and **P4** as a result of electron-donating alkoxy side chain. In contrast, the $\lambda_{e,max}$ of **P1**, **P2**, and **P3** were bathochromic shifted because of the effect of nitrogen of carbazole on the emission.

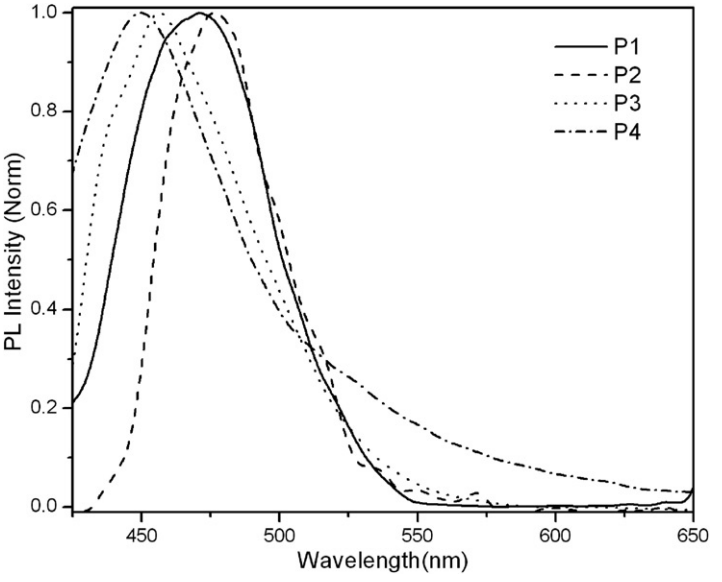

Figure 2. PL spectra of the polymers in DMF (10^{-5} mol L^{-1}).

3.3. *Thermal properties*

Thermal properties of polymers were obtained by TGA and DSC measurements and the results are tabulated in table 1. The TGA curves (Supplementary material) of polymers exhibit high thermal stability and the onset temperatures with 5% weight loss (T_d) of **P1**, **P2**, **P3,** and **P4** were 317°C, 327°C, 269°C, and 335°C under nitrogen, respectively. Synchronously, the glass transition temperatures (T_g) of **P1**, **P2**, **P3,** and **P4** were 98°C, 92°C, 116°C, and 105°C and no crystallization or melting peaks were detected, indicating that the polymers are amorphous. The high thermal stability of the polymers could benefit to increased stability of the DSSCs, preventing morphological change, deformation, and degradation of the active layer by current-induced heat during operation of the photovoltaic polymers [48].

3.4. *Electrochemical properties*

All CV values can be given by using a method based on adiabatic potential energy surfaces of both the donor and acceptors. CV is considered an effective tool in investigating electrochemical properties of conjugated compounds. The oxidation and reduction potentials revealed in cyclic voltammograms showed the highest occupied molecular orbital (HOMO) and lowest unoccupied molecular orbital (LUMO) levels, which correspond to ionization potentials and electron affinities, respectively. The polymer films coated on a glassy carbon working electrode, supported in 0.1 mol L^{-1} $[Bu_4N]BF_4$ (Bu = butyl) in anhydrous acetonitrile solution, were measured at a scanning rate of 50mV s^{-1}. The corresponding electrochemical data are listed in table 2. The cyclic voltammograms of the polymers are provided in

Table 2. Electrochemical properties of **P1–P4**.

Polymer	E^{ox}_{onset}(V)	E^{red}_{onset}(V)	HOMO (eV)	LUMO (eV)	E_g (eV)
P1	1.35	−1.14	−5.75	−3.26	2.49
P2	1.38	−1.16	−5.78	−3.24	2.54
P3	1.34	−1.01	−5.74	−3.39	2.35
P4	1.40	−1.20	−5.80	−3.20	2.60

"Supplementary material." When SCE electrode was used as the reference electrode, the correlation can be expressed as equations [49, 50]:

$$\text{HOMO} = -\text{e}\,(E_{ox} + 4.40)\ (\text{eV}),$$
$$\text{LUMO} = -\text{e}\,(E_{red} + 4.40)\ (\text{eV}).$$

The results show that the reduction and oxidation potentials of **P3** are $E_{red} = -1.01$ eV and $E_{ox} = 1.34$ eV, respectively. The energy band gap (E_g) was 2.35 eV, the energy value of the HOMO was calculated to be −5.74 eV and the LUMO was calculated to be −3.39 eV. For **P1**, **P2**, and **P4** the HOMO were calculated as −5.75 eV, −5.78 eV, and −5.80 eV, with an E_g of 2.49 eV, 2.54 eV, and 2.60 eV, respectively. **P2** exhibited a higher energy band gap than **P1** due to the steric effect. Incorporation of the arene groups into the main PF chain impacts the energy level of HOMO and LUMO, leading to the distinctive E_g in the polymers, which is valuable to make a deep study of solar cell materials.

On the basis of the CV data, the LUMO of the complexes follows the order **P3** < **P1** < **P2** < **P4**, which shows that the electron accepting ability of the complexes follows the order **P4** > **P2** > **P1** > **P3** [51]. E_g of the complexes follows the order **P3** < **P1** < **P2** < **P4**, so **P3** is more suitable for fabrication of optoelectronic devices than either **P1**, **P2**, or **P4** because a relatively low E_g can absorb light efficiently, important to improving power conversion efficiency [52]. Values of optical band gaps of **P1**, **P2**, **P3**, and **P4** are 2.42 eV, 2.51 eV, 2.30 eV, and 2.52 eV, respectively, according to figure 1. The electrochemical band gaps are higher than the optically determined ones for two reasons: first, this may be due to interface barrier for charge injection [53] and second, the excited state in conjugated polymers was viewed as a bound exciton. Formation of charge carriers required a higher energy of optical absorption, with no easy detection by linear optical spectroscopy [54].

3.5. *Photocurrent–voltage measurements*

Figure 3 shows current density–voltage (J–V) characteristics of the devices fabricated by **P1–P4**. The corresponding open-circuit voltage (V_{oc}), short-circuit current density (J_{sc}), fill factor (FF), and solar energy-to-electricity conversion efficiency (η) of the polymers for devices are listed in table 3. J_{sc}, V_{oc}, and FF of the device based on **P3** achieved 1.63 mA cm^{-2}, 0.69 eV, and 0.50 and power conversion efficiency (η) reached 0.56%. The DSSCs based on **P1**, **P2**, and **P4** obtained η values 0.34% (J_{sc} = 1.06 mA cm^{-2}, $V_{oc} = 0.56$ V, $FF = 0.56$), 0.29% ($J_{sc} = 0.69$ mA cm^{-2}, $V_{oc} = 0.59$ V, $FF = 0.61$), and 0.23% ($J_{sc} = 0.62$ mA cm^{-2}, $V_{oc} = 0.58$ V, $FF = 0.50$), respectively. The power conversion efficiency based on **P3** reached 0.56%, higher than that of the

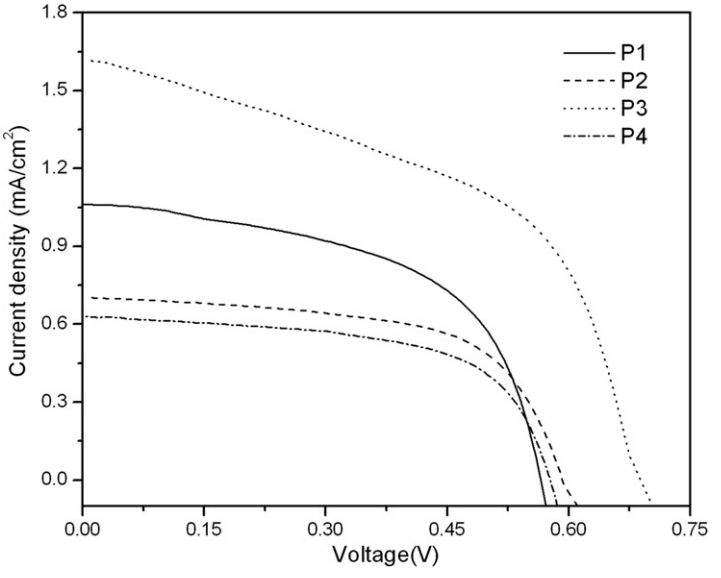

Figure 3. *J–V* curves of DSSCs based on **P1–P4** under simulated AM 1.5 G solar irradiation (100 mW cm^{-2}).

Table 3. Photovoltaic properties of DSSCs based on **P1–P4** under 1.5 G solar illumination.

Polymer	V_{oc} (V)	J_{sc} (mA cm^{-2})	*FF*	*H* (%)
P1	0.56	1.06	0.56	0.34
P2	0.59	0.69	0.61	0.29
P3	0.69	1.63	0.50	0.56
P4	0.58	0.62	0.60	0.23

devices based on **P1** (0.34%), **P2** (0.29%), and **P4** (0.23%). This is attributed to significant difference of the electron donor unit, with fluorene more suitable for donor unit than alkoxy benzene derivatives or carbazole derivatives.

The low J_{sc} is ascribed to weak adsorption onto the surface of TiO_2, low charge separation, the narrow absorption spectra of the polymers, and low transportation efficiency. The results indicate that modification of the dyes in terms of electron-donating monomers is an effective method to control J_{sc}. Moreover, a relatively high J_{sc} is very important to improve PCE. The J_{sc} of the DSSCs based on **P3** as the electron donor unit is the highest of the polymers and **P3** is more suitable for fabrication of optoelectronic devices than others. Film-forming and weak adsorption onto the surface of TiO_2 are two major factors that limit performance of DSSCs [55, 56]. Investigation is underway to optimize device performance.

4. Conclusions

We report synthesis and characterization of four polymeric metals with the same Cd(II) complex in the side chain and different conjugated backbone structures. The four

materials have good thermal stability, good open-circuit voltages and fill factors but moderate power conversion. We have found that the conjugated backbone containing fluorene benefits ICT increases the generation of photocurrent. The η of **P1–P4** are 0.34%, 0.29%, 0.56%, and 0.23%, respectively, suggesting further optimization is essential before application in DSSCs.

To obtain outstanding η, there are still many challenges. First, J_{sc} based on all the materials is very low due to low adsorption affinities on the TiO_2; anchoring groups such as $-CN$, $-COOH$, or $-SO_3H$ should be introduced in the structure. Structural optimization with broad spectral coverage and excellent charge separation and transportation are expected to produce more efficient photosensitive dyes. Our work in these directions is underway.

References

[1] A. Goetzberger, C. Hebling, H.W. Schock. *Mater. Sci. Eng. R.*, **40**, 1 (2003).
[2] B. O'Reagen, M. Grätzel. *Nature*, **353**, 737 (1991).
[3] M.J. Grätzel. *Photochem. Photobiol. A*, **168**, 235 (2004).
[4] M.K. Nazeeruddin, S. Fantacci, A. Selloni, G. Viscardi, P. Liska, S. Ito, B. Takeru, M. Grätzel. *J. Am. Chem. Soc.*, **127**, 16835 (2005).
[5] J. Wiberg, T. Marinado, D.P. Hagberg, L. Sun, A. Hagfeldt, B. Albinsson. *J. Phys. Chem. C*, **113**, 3881 (2009).
[6] K. Hara, M. Kurashige, S. Ito, A. Shinpo, S. Suga, K. Sayama, H. Arakawa. *Chem. Commun.*, 252 (2003).
[7] W. Zeng, Y. Cao, Y. Bai, Y. Wang, Y. Shi, M. Zhang, F. Wang, C. Pan, P. Wang. *Chem. Mater.*, **22**, 1915 (2010).
[8] L. Schmidt-Mende, U. Bach, R. Humphry-Baker, T. Horiuchi, H. Miura, S. Ito, S. Uchida, M. Grätzel. *Adv. Mater.*, **17**, 7 (2005).
[9] E.M. Barea, R. Caballero, F. Fabregat-Santiago, P. de la Cruz, F. Langa, J. Bisquert. *Chem. Phys. Chem.*, **10**, 1 (2009).
[10] K. Hara, K. Sayama, Y. Ohga, A. Shinpo, S. Suga, H.A. Arakawa. *Chem. Commun.*, 569 (2001).
[11] L. Schmidt-Mende, U. Bach, R. Humphry-Baker, T. Horiuchi, H. Miura, S. Ito. *Adv. Mater.*, **17**, 813 (2005).
[12] K.R.J. Thomas, J.T. Lin, Y.C. Hsu, K.C. Ho. *Chem. Commun.*, 4098 (2005).
[13] S. Yahagida, G.K.R. Senadeera, K. Nakamura, T. Kitamura, Y. Wada. *J. Photochem. Photobiol. A: Chem.*, **166**, 75 (2004).
[14] J.K. Mwaura, X. Zhao, H. Jiang, K.S. Schanze, J.R. Reynolds. *Chem. Mater.*, **18**, 6109 (2006).
[15] W. Zhang, Z. Fang, M.J. Su, M. Saeys, B. Liu. *Macromol. Rapid Commun.*, **30**, 1533 (2009).
[16] Y.J. Liu, X. Guo, N. Xiang, B. Zhao, H. Huang, H. Li. *J. Mater. Chem.*, **20**, 1140 (2010).
[17] K.R. Thomas, J.T. Lin, Y.C. Hsu, K.C. Ho. *Chem. Commun.*, 4098 (2005).
[18] N. Cho, H. Choi, D. Kim, K. Song, M.S. Kang, S.O. Kang, J. Ko. *Tetrahedron*, **65**, 6236 (2009).
[19] D. Heredia, J. Natera, M. Gervaldo, L. Otero, F. Fungo, C.Y. Lin. *Org. Lett.*, **12**, 12 (2010).
[20] H. Tian, X. Yang, J. Cong, R. Chen, J. Liu, Y. Hao, A. Hagfeldt, L. Sun. *Chem. Commun.*, 6288 (2009).
[21] U. Scherf, E.J.W. List. *Adv. Mater.*, **14**, 477 (2002).
[22] E. Bundgaard, F.C. Krebs. *Sol. Energy Mater. Sol. Cells*, **91**, 954 (2007).
[23] R. Kroon, M. Lenes, J.C. Hummelen, P.W.M. Blom. *Polym. Rev.*, **48**, 531 (2008).
[24] H.H. Fong, A. Papadimitratos, G.G. Malliaras. *Appl. Phys. Lett.*, **89**, 172 (2006).
[25] M. Chiesa, L. Burgi, J.S. Kim, R. Shikler, R.H. Friend, H. Sirringhaus. *Nano Lett.*, **5**, 559 (2005).
[26] T. Yohannes, F. Zhang, M. Svensson, J.C. Hummelen, M.R. Andersson, O. Inganas. *Thin Solid Films*, **449**, 152 (2004).
[27] A. Gadisa, W. Mammo, L.M. Andersson, S. Admassie, F. Zhang, M.R. Andersson, O. Inganas. *Adv. Funct. Mater.*, **17**, 3836 (2007).
[28] J. Roncali. *Macromol. Rapid Commun.*, **28**, 1761 (2007).
[29] B.C. Thompson, M.J. Frechet. *Angew. Chem. Int. Ed.*, **47**, 58 (2008).
[30] M.M. Wienk, M.P. Struijk, R.A.J. Janssen. *Chem. Phys. Lett.*, **422**, 488 (2006).
[31] T. Taima, M. Chikamatsu, Y. Yoshida, K. Saito, K. Yase. *Appl. Phys. Lett.*, **85**, 6412 (2004).
[32] A. Saylam, Z. Seferoglu, N. Ertan. *Dyes Pigm.*, **76**, 470 (2008).

[33] C.H. Chen, J.M. Shi. *Coord. Chem. Rev.*, **171**, 161 (1998).
[34] G.R. Clemo, R. Howe. *J. Chem. Soc., Dalton Trans.*, 3552 (1955).
[35] L.F. Xiao, Y. Liu, Q. Xiu, L.R. Zhang, C.F. Zhong. *Tetrahedron*, **66**, 2835 (2010).
[36] Y. Zhou, C.F. Zhong, Y. He, L.F. Xiao, H.L. Zhang. *J. Inorg. Organomet. Polym.*, **19**, 328 (2009).
[37] M.K. Nazeeruddin, A. Kay, I. Rodicio, R. Humphry-Baker, E. Mueller, P. Liska. *J. Am. Chem. Soc.*, **115**, 6382 (1993).
[38] G.R.A. Kumara, S. Kaneko, A. Konno, M. Okuya, K. Murakami. *Prog. Photovoltaics Res. Appl.*, **14**, 643 (2006).
[39] K.L. Handoo, K. Gadru. *Ind. J. Chem.*, 909 (1983).
[40] L.F. Xiao, Y. Liu, Q. Xiu, L.R. Zhang, C.F. Zhong. *J. Polym. Sci. Pol. Chem.*, **48**, 1943 (2010).
[41] B.K. An, Y.H. Kim, D.C. Shin. *Macromolecules*, **34**, 3993 (2001).
[42] A. Saylam, Z. Swferoglu, N. Ertan. *Dyes Pigm.*, **76**, 470 (2008).
[43] J.H. Hou, L.J. Huo, C. He, C.H. Yang, Y.F. Li. *Macromolecular*, **39**, 601 (2006).
[44] L.D. Massimo, G. Annarita, A. Iolinda, C. Alessandra, G. Mauro, B. Sandra. *Dalton Trans.*, 2424 (2004).
[45] C. Baskar, Y.H. Lai, S. Valiyaveettil. *Macromolecules*, **34**, 6258 (2001).
[46] G. Robert, H. Charles, R. Freiser, L. Friedel, E. Hilliard, W.D. Johnston. *Spectrochim. Acta*, **8**, 1 (1956).
[47] R. Pagadala, P. Ali, J.S. Meshram. *J. Coord. Chem.*, **62**, 4015 (2009).
[48] S. Bertho, I. Haeldermans, A. Swinnen, W. Moons, T. Martens, L. Lutsen, D. Vanderzande, J. Manca. *Sol. Energy Mater. Sol. Cells*, **91**, 385 (2007).
[49] N.S. Cho, D.H. Hwang, B.J. Jung. *Macromolecules*, **37**, 5265 (2004).
[50] T. Bessho, E.C. Constable, M. Graetzel, A. Hernandez Redondo, C.E. Housecroft, W. Kylberg, Md.K. Nazeeruddin, M. Neuburger, S. Schaffner. *Chem. Commun.*, 3717 (2008).
[51] Y. Sun, S. Wang. *Inorg. Chem.*, **48**, 3755 (2009).
[52] Y.J. Cheng, S.H. Yang, C.S. Hsu. *Chem. Rev.*, **109**, 5868 (2009).
[53] K.A. Barve, S.S. Raut, A.V. Mishra, V.R. Patil. *J. Appl. Polym. Sci.*, **122**, 3483 (2011).
[54] T. Johansson, W. Mammo, M. Svensson, M.R. Andersson, O. Inganas. *J. Mater. Chem.*, **13**, 1316 (2003).
[55] K. Hara, T. Sato, R. Katoh, A. Furube, T. Yoshihara, M. Murai, M. Kurashige, S. Ito, A. Shinpo, S. Suga, H. Arakawa. *Adv. Funct. Mater.*, **15**, 246 (2005).
[56] S.L. Li, K.J. Jiang, K.F. Shao, L.M. Yang. *Chem. Commun.*, 2792 (2006).